Supporting information for: Modeling Electron Transfer in Diffusive Multidimensional Electrochemical Systems

Alec J. Coffman,*,† Aparna Karippara Harshan,‡ Sharon Hammes-Schiffer,¶ and Joseph E. Subotnik†

Department of Chemistry, University of Pennsylvania, Philadelphia, Pennsylvania 19104, USA, Department of Chemistry, University of Illinois at Urbana-Champaign, Urbana, Illinois 61801, USA, and Department of Chemistry, Yale University, New Haven, Connecticut 06520, USA

E-mail: alecja@sas.upenn.edu

*To whom correspondence should be addressed
†Department of Chemistry, University of Pennsylvania, Philadelphia, Pennsylvania 19104, USA
‡Department of Chemistry, University of Illinois at Urbana-Champaign, Urbana, Illinois 61801, USA
¶Department of Chemistry, Yale University, New Haven, Connecticut 06520, USA

Appendix A: Stencil details for 2D simulations

When simulating 2D voltammetry experiments using the diagonalized Fokker-Planck operator, one requires a high order of accuracy for approximating the second derivative calculation with respect to ζ. To achieve convergent results using this approach, a higher order second derivative stencil was utilized. Specifically, we used a centered difference, 17-stencil, which is accurate to sixteenth order with respect to the grid spacing in ζ, $\mathcal{O}(d\zeta^{16})$. For calculating the derivative at grid point ζ_i the stencil contains the points $[\zeta_i - 8d\zeta, \zeta_i + 8d\zeta]$, with weights calculated by elimination of lower order error terms using the Taylor expansions of $[\zeta_i - 8d\zeta, \zeta_i + 8d\zeta]$.[S1] For the x-direction, we used a simple 3-stencil with points $[x_i - dx, x_i, x_i + dx]$ for points x_i.

Appendix B: The transition from a separable to a non-separable Hamiltonian

In figures 8 and 9 we plot results for the case that $\zeta_A(x) \approx \zeta_A^0$ at $x = 0$ and $\zeta_A(x) \approx \zeta_A^\infty$ for $x \neq 0$ (see equation 39). In practice, this choice of $\zeta_A(x)$ corresponds to choosing a sufficiently large value of σ for the analytical expression, $\zeta_A(x) = (\zeta_A^0 - \zeta_A^\infty)e^{-\sigma x^2} + \zeta_A^\infty$. Thus, in this limit, the x and ζ directions are far from separable: the reorganization energy (characterizing the shift of ζ as a function of charge states) depends critically and dramatically on the distance to the metal (x).

Now, that being such, one can increase separability by choosing a smaller value of σ (see equation 39), so that the reorganization energy changes more slowly as a function of x. To that end, in figure S1 we plot (on the left) linear sweep voltammograms for different σ values and (on the right) the well minimum position ζ_A as a function of the grid point in x, x_i. For small σ values, where there is little difference between $\zeta_A(x)$ values at the first few grid points, we find that the 1D MH model and the full 2D model agree quantitatively. This

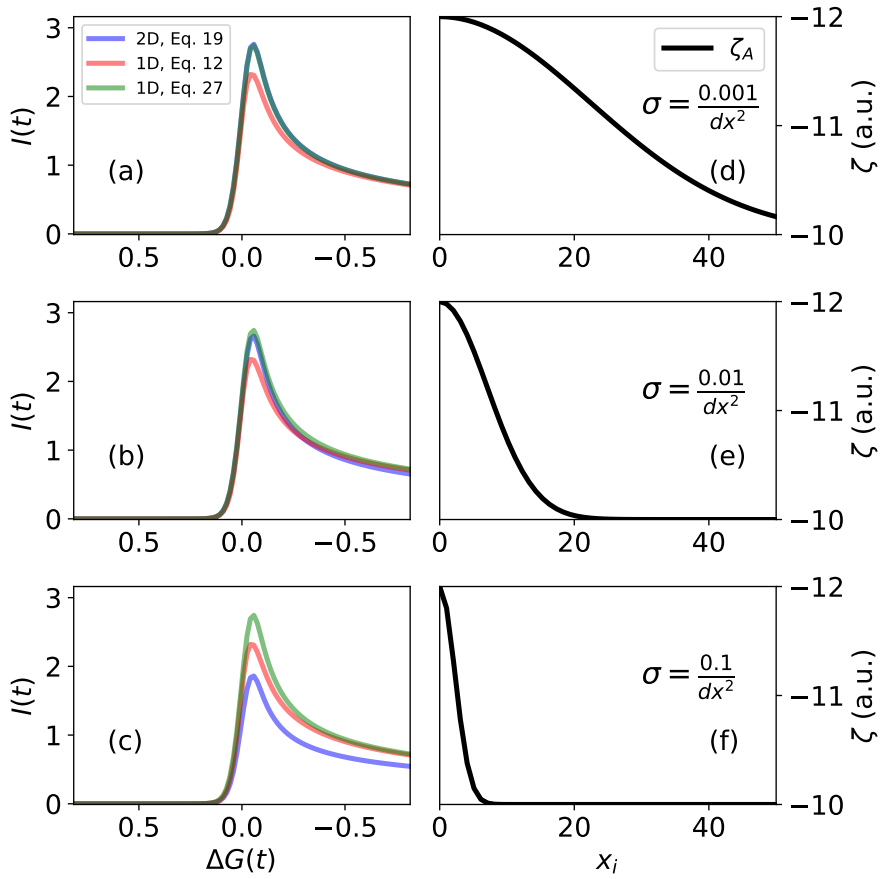


Figure S1: (left) Linear sweep voltammograms and (right) ζ_A positions as a function of x for different σ values in $\zeta_A(x)$ (see equation 39). $\Delta G_i = 0.816$ V, $\Delta G_f = -0.816$ V, $\zeta_A^0 = -6.35$ Å (-12 a.u.), $\zeta_A^\infty = -5.29$ Å (-10 a.u.), $D = 5.5 \cdot 10^{-4}$ cm^2/sec, $\omega = 1.03 \cdot 10^{13}$ sec^{-1}, $\lambda_0 = 31.84kT$, $\frac{\Gamma}{\hbar} = 1.40 \cdot 10^9$ cm/sec, and $\nu = 112$ V/sec for each subplot. (a) & (d) $\sigma = \frac{0.001}{dx^2}$, (b) & (e) $\sigma = \frac{0.01}{dx^2}$, (c) & (f) $\sigma = \frac{0.1}{dx^2}$. For small σ values, where ζ_A depends slowly on x and motion in x and ζ is largely separable, we see quantitative agreement between the 1D MH and 2D models. However, for large σ values, where there is no separability, the 1D MH and 2D models do not agree.

results confirms our intuition: the full 2D dynamics can be reduced to 1D when the x and ζ directions are close to separable.

Appendix C: Implementation of 1D BV and Nernstian boundary conditions

For Nernstian dynamics (equation 4) and Butler-Volmer dynamics (equations 5 and 6) there are two unknowns ($c_A(x=0)$ and $c_B(x=0)$) at the surface, but only one equation. As such, one additional equation is needed. To that end, it is standard[S2] to use the additional constraint that the flux of species A and B are equal and opposite at the boundary,

$$J_A|_{x=0} = D_A^x \frac{\partial c_A}{\partial x}|_{x=0} = k_f c_A|_{x=0} - k_b c_B|_{x=0} \tag{1a}$$

$$J_B|_{x=0} = D_B^x \frac{\partial c_B}{\partial x}|_{x=0} = -k_f c_A|_{x=0} + k_b c_B|_{x=0}. \tag{1b}$$

Using a 2 stencil with a forward difference approximation for the spatial derivatives ($\frac{\partial c_i}{\partial x} = \frac{c_{i,1}-c_{i,0}}{dx}$ for species i), one can arrive at the following boundary values for Nernstian dynamics:

$$c_{A,0} = \frac{c_{B,1} + \frac{D_A^x}{D_B^x} c_{A,1}}{\frac{D_A^x}{D_B^x} + e^{-\beta \Delta G}} \tag{2a}$$

$$c_{B,0} = c_{A,0} e^{-\beta \Delta G}, \tag{2b}$$

and for Butler-Volmer dynamics:

$$c_{A,0} = \frac{c_{B,1} k_b dx + D_A^x c_{A,1}(1 + \frac{k_b dx}{D_B^x})}{D_A^x + dx(k_f + \frac{D_A^x}{D_B^x} k_b)} \tag{3a}$$

$$c_{B,0} = c_{B,1} + \frac{D_A^x}{D_B^x}(c_{A,1} - c_{A,0}). \tag{3b}$$

References

(S1) Keller, H. B.; Pereyra, V. Symbolic Generation of Finite Difference Formulas. *Math. Comput.* **1978**, *32*, 955–971.

(S2) Bard, A. J.; Faulkner, L. R. *Electrochemical Methods: Fundamentals and Applications*; Wiley: New York, 2001.